Single cell analysis of autism patient with bi-allelic NRXN1-alpha deletion reveals skewed fate choice in neural progenitors and impaired neuronal functionality

Lam, Matti; Moslem, Mohsen; Bryois, Julien; Pronk, Robin J; Uhlin, Elias; Ellström, Ivar Dehnisch; Laan, Loora; Olive, Jessica; Morse, Rebecca; Rönnholm, Harriet; Louhivuori, Lauri; Korol, Sergiy V; Dahl, Niklas; Uhlén, Per; Anderlid, Britt-Marie; Kele, Malin; Sullivan, Patrick F; Falk, Anna

Published in:
Experimental Cell Research

DOI:
10.1016/j.yexcr.2019.06.014

2019

Document Version:
Publisher's PDF, also known as Version of record

Experimental Cell Research 383 (2019) 111469

Contents lists available at ScienceDirect

Experimental Cell Research

journal homepage: www.elsevier.com/locate/yexcr

Single cell analysis of autism patient with bi-allelic *NRXN1-alpha* deletion reveals skewed fate choice in neural progenitors and impaired neuronal functionality

Matti Lam[a], Mohsen Moslem[a,1], Julien Bryois[b,1], Robin J. Pronk[a], Elias Uhlin[a], Ivar Dehnisch Ellström[c], Loora Laan[e], Jessica Olive[a], Rebecca Morse[a], Harriet Rönnholm[a], Lauri Louhivuori[c], Sergiy V. Korol[f], Niklas Dahl[e], Per Uhlén[c], Britt-Marie Anderlid[d], Malin Kele[a], Patrick F. Sullivan[b], Anna Falk[a,*]

[a] Department of Neuroscience, Karolinska Institutet, Stockholm, Sweden
[b] Department of Medical Epidemiology and Biostatistics, Karolinska Institutet, Stockholm, Sweden
[c] Department of Medical Biochemistry and Biophysics, Karolinska Institutet, Stockholm, Sweden
[d] Department of Molecular Medicine and Surgery, Karolinska Institutet, Stockholm, Sweden
[e] Department of Immunology, Genetics and Pathology, Science for Life Laboratory, Uppsala University, Uppsala, Sweden
[f] Department of Neuroscience, Uppsala University, Uppsala, Sweden

ARTICLE INFO

Keywords:
Autism spectrum disorder
Neurexin
Neurexin-1 alpha
Induced pluripotent stem cell
Neural stem cell
Single cell RNA sequencing
Neural development
Disease modeling

ABSTRACT

We generated human iPS derived neural stem cells and differentiated cells from healthy control individuals and an individual with autism spectrum disorder carrying bi-allelic *NRXN1-alpha* deletion. We investigated the expression of *NRXN1-alpha* during neural induction and neural differentiation and observed a pivotal role for *NRXN1-alpha* during early neural induction and neuronal differentiation. Single cell RNA-seq pinpointed neural stem cells carrying *NRXN1-alpha* deletion shifting towards radial glia-like cell identity and revealed higher proportion of differentiated astroglia. Furthermore, neuronal cells carrying *NRXN1-alpha* deletion were identified as immature by single cell RNA-seq analysis, displayed significant depression in calcium signaling activity and presented impaired maturation action potential profile in neurons investigated with electrophysiology. Our observations propose *NRXN1-alpha* plays an important role for the efficient establishment of neural stem cells, in neuronal differentiation and in maturation of functional excitatory neuronal cells.

1. Introduction

Autism spectrum disorders (ASD) are a set of heterogeneous neurodevelopmental conditions that affect ~1% of worldwide population [1] with important personal, familial, economic, and societal burdens [2]. Symptoms include impairments in social interaction and communication, with accompanying restricted or repetitive behaviors, activities, or obsessive interests [3]. ASD has strong and complex genetic architecture with more than 100 associated loci or chromosomal abnormalities [4]. Among them, multiple genes in the neurexin family are known to be involved in ASD [5] and schizophrenia [6]. Neurexins have been studied specifically in synapse formation and synaptic plasticity during neural development. They are cell adhesion molecules in the presynaptic cell membrane in both excitatory and inhibitory synapses and play an important role in calcium-dependent transmission in the central and peripheral nervous system (for review see Ref. [7]). Neurexin 1 (*NRXN1)* is transcribed from multiple different promoters, but has two predominant isoforms, the longer *NRXN1-alpha* (*NRXN1-a*) and shorter C-terminal *NRXN1beta* (*NRXN1-b*) [8,9]. *NRXN1-a* isoforms preferentially bind to a variety of trans-synaptic partners, including neuroligins, cerebellins, neurexophilins, and leucine-rich repeat transmembrane proteins each of which serve different synaptic functions [7,10].

Rare copy number variants impacting combinations of exons in *NRXN1-a* have been associated with ASD and schizophrenia [11] and appears to exert an impact on disease phenotype [6,10]. Several studies have developed animal and cellular models to acquire an in-depth perspective on *NRXN1-a* functionality and co-interactors. Mouse studies

* Corresponding author. Karolinska Institutet, Department of Neuroscience, 171 77 Stockholm, Sweden.
E-mail address: Anna.Falk@ki.se (A. Falk).
[1] Equal contribution.

https://doi.org/10.1016/j.yexcr.2019.06.014
Received 20 May 2019; Received in revised form 31 May 2019; Accepted 11 June 2019
Available online 12 July 2019

revealed deletion of pan-neurexin-alphas (*Nrxn1-a*, *Nrxn2-a*, *Nrxn3-a)* impaired both spontaneous and evoked Ca^{2+} triggered neurotransmitter release in excitatory and inhibitory synapses in the brainstem and neocortex [12]. Further, *Nrxn1-a* deficient mice have impaired excitatory synaptic transmission in the hippocampus but no significant alterations in social behaviors or in spatial learning [13].

Additionally, mice with pan-neurexin deletion maintain normal synapses numbers but show a massive impairment in action potential-induced calcium influx in neurons [14]. Moreover, comparison of *Nrxn1-a* double-knockout mice and human cellular models established by introducing heterozygous mutation into *NRXN1-a* revealed that hetero- or homozygous mutation of murine *Nrxn1-a* have no significant effects on functional characteristics of cortical neurons while heterozygous mutation of human *NRXN1-a* impairs neurotransmitter release and frequency of spontaneous evoked excitatory postsynaptic currents in embryonic stem cell-derived induced neurons [5]. These studies indicated the importance of *NRXN1-a* in human development, cognition and intellectual activities and also highlighted the need for a specific cell model with complete absence of *NRXN1-a* to identify its impact and also its potential partners in human neurogenesis.

Here, we took advantage of iPS cell technology [15,16] to generate a iPS cell model from an individual with autism spectrum disorder carrying bi-allelic *NRXN1-a* deletion (del) [17]. From these iPS cells we derived neuroepithelial stem (NES) cells and performed single cell RNA sequencing [18] to shed light on gene expression patterns affected by *NRXN1-a* del during neuronal differentiation.

2. Results

2.1. Cellular model of early and late neuronal development display two waves of NRXN1 expression

iPS cells from an individual diagnosed with ASD carrying bi-allelic *NRXN1-a* del [17] and healthy control individuals (Ctrl-7, Ctrl-3, Ctrl-9, Ctrl-10) [19–21] were generated from skin fibroblasts, induced toward neuroepithelial stem (NES) cells [22] and further spontaneously differentiated to neurons for 28 days (DIFF), 49 days and 70–75 days (Fig. 1A). Established iPS cells were characterized pluripotent by morphology, positively stained for OCT4 and NANOG, microarray transcriptomes were probed for pluripotency markers, analyzed by Pluritest [23] and the iPS cell lines showed stable karyotype (Figs. S1A–S1E, for Ctrl-7, Ctrl-9, Ctrl-10, Ctrl-3 see Refs. [19–21])).

Healthy control NES and *NRXN1-a* del NES cells were established with a modified dual SMAD inhibition protocol [24]. During neural induction we observed a complete absence of *NRXN1-a* expression in *NRXN1-a* del iPS cells, while in the same time interval *NRXN1-a* doubled in healthy control cells at day 2 and gradually decreased until day 12 at capture of NES cells (Fig. 1B). We also observed this pattern of *NRXN1* expression peaking during neural induction in Cortecon (http://cortecon.neuralsci.org) [25] (Fig. S1F). Additionally, when we probed single cell RNA-seq data of human preimplantation embryo [26] we also noticed *NRXN1* expressed during early embryonic development (Fig. S1G). These combined observations suggest *NRXN1-a* possessing a developmentally earlier function rather than only acting in the synapse.

Despite differences of *NRXN1* expression in healthy control cells and *NRXN1-a* del cells during neural induction, established NES cells from both healthy individuals and *NRXN1-a* del individual appeared growing in organized rosette-like morphology with apical distribution of the cell surface marker ZO1. The NES cells stained positive for broad neural stem cell markers such as NESTIN, SOX2, PLZF and furthermore, we did not detect significant differences in spontaneous calcium signaling activity (Fig. 1C, Fig. S1H, Fig. S1I). These combined observations suggested we had established stable NES cell lines.

To our surprise, when measuring newly synthesized DNA by incorporation of EdU to assess cell cycle phases, we observed a significant higher percentage of EdU negative *NRXN1-a* del NES cells in G0/G1-phase, indicating a slower proliferation rate than Ctrl-7 NES, while simultaneously observing a significant higher percentage of EdU positive Ctrl-7 NES cells in G2 phase. (Fig. 1D). Similarly, when we counted cells for proliferation marker Ki-67, higher proportions were observed in Ctrl-7 NES cells thus indicating a slower proliferation rate in *NRXN1-a* del NES cells (Fig. S1J). These differences in proliferation suggested to us that cell identity in *NRXN1-a* del NES cells might be altered.

Probing for *NRXN1-a* expression in healthy NES cells undergoing differentiation by growth factor removal, we detected a ramping up of expression from nearly no levels to robust upregulation upon 28 days of differentiation. Meanwhile as expected, we neither detected mRNA or protein of *NRXN1-a* in *NRXN1-a* del DIFF cells (Fig. 1E and F). Curiously, we did not observe obvious neuronal differentiation differences between Ctrl-7 DIFF and *NRXN1-a* del DIFF morphology (Fig. 1G). These superficial observations lead us to consider neuronal differentiation also functions under other compensatory mechanisms not entirely dependent on presence of *NRXN1-a* expression in the neurons.

To investigate whether *NRXN1-a* expression during early neuronal development influences neuronal differentiation, we took a transcriptomics approach [18] and obtained Single cell RNA-seq from 984 high quality single cells that were used for analysis at the NES cell stage and DIFF cell stage (Fig. 1A schematic single cells). In our single cell data we verified high *NRXN1* expression in Ctrl-7 DIFF single cells and low expression of *NRXN1* in *NRXN1-a* del DIFF single cells (Fig. 1H). Thus reflecting our observations in the bulk sample qPCR. Similarly, when looking at genes related to proliferation, we observed fewer *NRNX1-a* del NES cells compared to Ctrl-7 NES cells (Fig. 1I). In single cell transcripts mapped to the genomic region of *NRXN1*, again we confirmed *NRXN1-a* long transcript expression in Ctrl-7 DIFF cells and exclusive expression of *NRXN1-b* short transcript in *NRXN1-a* del DIFF cells (Fig. S1K). These combined observations strongly indicate a complete absence of *NRXN1-a* in *NRXN1-a* del cells.

Our unexpected observations of *NRXN1* expression during developmentally early time points agree with recent studies showing similar *NRXN1* expression patterns in various types of radial glia cells and neuronal cell types of human fetal brain during embryonic development (http://linnarssonlab.org/ventralmidbrain/and https://bitly.com/cortexSingleCell) [27,28]. In addition, slower proliferation rate has previous been reported to be indicative of shifting identity in fetal neural stem cells [29,30].

2.2. NRXN1-a deletion alters outcome of cell identity in established NES and DIFF cells

We used BackSPIN [31], a bi-clustering algorithm on single cells for both Ctrl-7 and *NRXN1-a* del NES and DIFF to identify the 2000 most variable genes across 984 single cell transcriptomes to identify cell types present in our single cell RNA-seq experiment (Table S1). As expected, we observed that both NES and DIFF cells consisted of various cell types appearing during early and late neurogenesis. Four cell types were identified among NES cells: neural stem cells, radial glia-like cells, intermediate progenitors (IP) for neurons and IP for astroglia. In DIFF cells we identified another four cell types namely immature neurons, immature astroglia, neurons and astroglia (Fig. 2A), these cells appeared in line with expected outcome of differentiation [32].

We visualized the identified cell types in tSNE plot [33] and observed reasonable separation ranging from NES to DIFF cells with little overlap (Fig. 2B). Further, we observed sample conditions separating Ctrl-7 and *NRXN1-a* del cells (Fig. 2C). Looking into the NES and DIFF cell contribution in cell types, we found significant differences ($\chi^2 = 1283.4$, df = 21, p-value < 2.2e-16) with Ctrl-7 cells consisting mostly of neural stem cells, intermediate progenitors and neurons. In contrast to cell types representing Ctrl-7 cells, *NRXN1-a* del cells consisted of radial glia-like cells, immature neurons and astroglia (Fig. 2D). We found highly enriched genes in each cell type, *GJA1, HIST1H3C, WNT4* in neural stem cells, *MAGEL2, SNCG, CDKN1A* in IP for neurons,

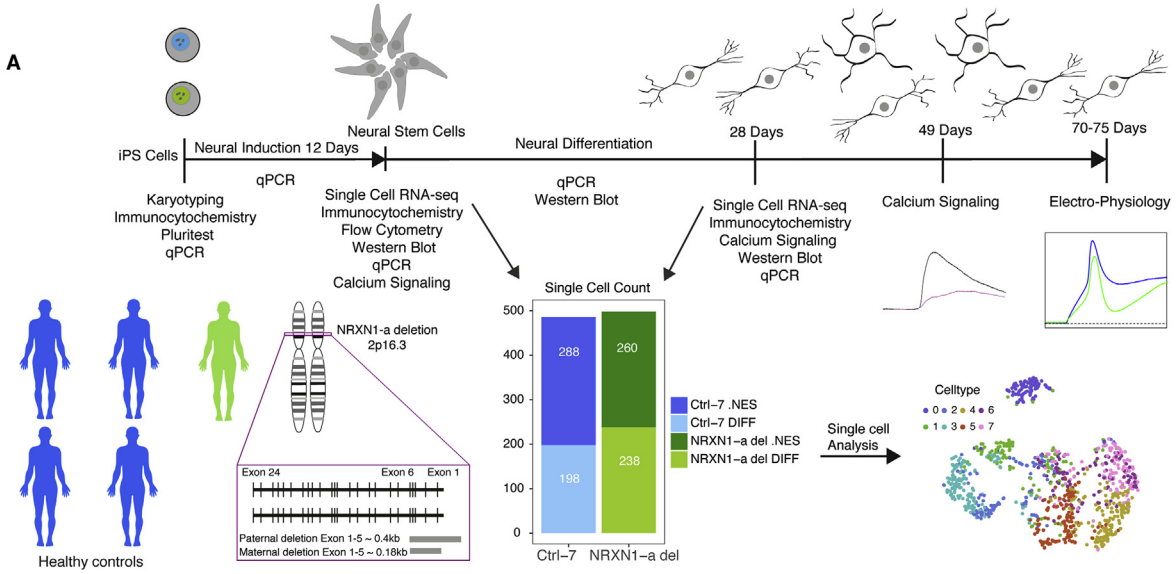

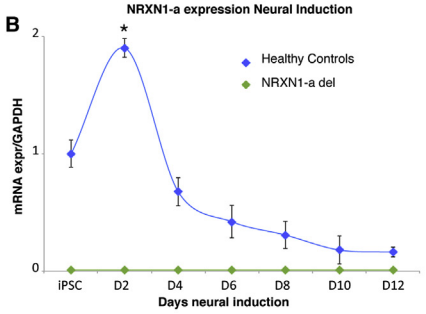

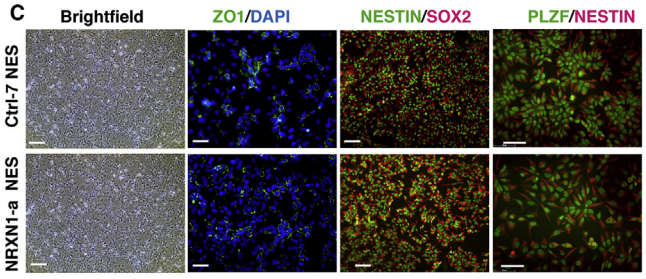

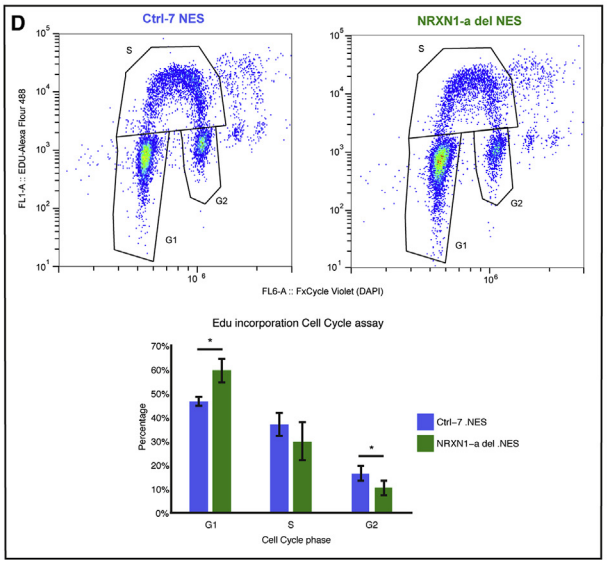

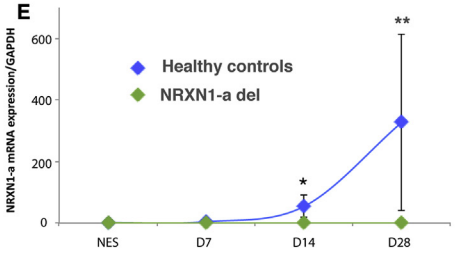

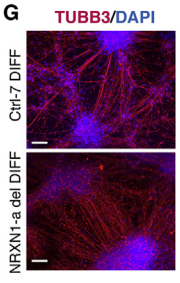

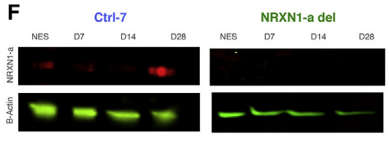

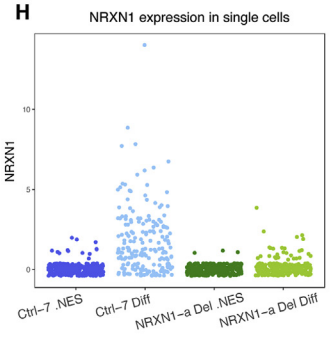

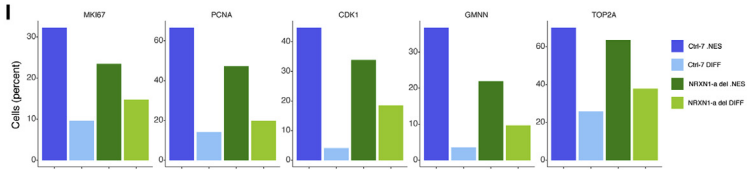

(caption on next page)

Fig. 1. Establishment of neural stem cells and neuronal differentiation display *NRXN1-a* expressed twice during development. A) Experimental overview, iPS cells and NES cells established from individuals, samples from neural stem cells and differentiated cells collected for single cell RNA-seq. *B) NRXN1-a* gene expression during neural induction, *NRXN1-a* expression in three control iPS cells (Ctrl-7, Ctrl-9 and Ctrl-10) peak around day 2 and gradually decrease until NES cells are established, *NRXN1-a* is completely absent in *NRXN1-a* del iPS cells during neural induction. * Significant difference to iPS cells with p-value ≤ 0.05. C) NES cell morphology displayed in brightfield and immunocytochemistry staining for neural stem cell markers in ZO1, NESTIN, SOX2 and PLZF for Ctrl-7 and *NRXN1-a* del NES cells. No obvious differences observed between individuals, scalebar: 50 μm. D) EdU incorporation assay quantified by FACS representative images, 10.000 events were recorded (n = 3), barplot shows *NRXN1-a* del NES cells have lower EdU incorporation and more cells in G0/G1 phase (p-value < 0.001) while control NES cells (Ctrl-7 and Ctrl-10 (data not shown)) have higher EdU incorporation and more cells in G2 phase (p-value < 0.05) indicating lower proliferation rate in *NRXN1-a* del NES cells. *E) NRXN1-a* gene expression during neural differentiation for 28 days, three control NES lines (Ctrl-7, Ctrl-9 and Ctrl-10) DIFF cells gradually expresses higher levels of *NRXN1-a* while *NRXN1-a* del DIFF do not. N = 3. * P-Value ≤ 0.05. ** P-Value ≤ 0.001. F) NRXN1-a protein probe with Western blot during 28 days of differentiation (NES cells, Day 7, Day 14 and Day 28), NRXN1-a detected in Ctrl-7 DIFF cells while no protein is seen in *NRXN1-a* del DIFF cells. G) Beta-3 tubulin immunocytochemistry staining in Ctrl-7 DIFF cells and *NRXN1-a* del DIFF cells showed no obvious differences, scalebar: 50 μm. *H) NRXN1* expression in 984 single cells, observation of *NRXN1* expressed in Ctrl-7 DIFF cells and *NRXN1-a* del DIFF cells. I) Barplots for presence of proliferation markers (*MKI67*, *PCNA*, *CDK1*, GMNN, *TOP2A*) in single cell transcriptomes display more expression in Ctrl-7 NES cells compared to *NRXN1-a* del NES cells.

CNTN2, DLL3, NEUROG1 in immature neurons and *MYT1L, NRXN1, RTN1* in neurons (Fig. 2E–H). Similarly, we found *PAX6, HES5, SOX3* in radial glia-like cells, *AQP4, CALB1, NPY* in IP for astroglia, *CLU, ENKUR, SLIT3* in immature astroglia and *APOE, CD44, TNC* in astroglia (Fig. 2I-L). Comparing genes in our identified cell types to fetal brain cells during development [27,28] we saw NES cells expressing *GJA1, HIST1H3C, CNTN2, NEUROG1, NRXN1* and *MYT1L* reaffirmed neuronal fate choice while radial glia-like cells expressing *HES5, PAX6, SOX3, APOE, CD44* and *TNC* reaffirmed astroglia (non-neuronal) fate choice (Figs. S2A and S2B). Taken together, these observations indicated *NRXN1-a* deletion affects establishment of NES cells, since we observed skewed cell type distribution between Ctrl-7 and *NRXN1-a* del cells in the outcome of established neural progenitors, intermediate progenitors, differentiating neuronal cells and non-neuronal cells.

2.3. Pseudotime and trajectory modeling reveal NRXN1-a deletion results in higher proportion of astroglia in differentiated cells

Recognizing the inherent character of unsynchronized non-directed differentiation in our NES cell differentiation protocol, we used Monocle 2 [34] to order single cells in pseudotime. Pseudotime and trajectory projection placed all NES and DIFF cells along a differentiation trajectory starting from neural stem cells and ending in differentiated cells (Fig. 3A). We observed during differentiation cells choose two distinctly different fates and differentiated either into neurons or astroglia (Fig. 3B, S3A and Table 2).

When we plotted trajectory according to sample conditions, distinct patterns of distribution emerged along the projected trajectory between the Ctrl-7 DIFF and *NRXN1-a* del DIFF cells. Ctrl-7 DIFF cells aggregated into the neuron branch while *NRXN1-a* del DIFF cells spread out across all three branches (Fig. 3C). Hence, our observation suggests healthy control DIFF cells mainly differentiate into neurons while approximately half of *NRXN1-a* del DIFF cells differentiate towards neurons and remaining cells differentiate towards astroglia. (Fig. S3B). Estimating the proportion of cell fate commitment, we plotted identified cell types onto pseudotime trajectory backbone and observed at each stage of the differentiation process differences between control cells and *NRXN1-a* del cells. We observed how individual's contributed to cell types and observed neural stem cell contained mostly Ctrl-7 NES cells with a small fraction of *NRXN1-a* del NES cells, while radial glial-like cells contained mostly *NRXN1-a* del NES cells with a small fraction of *NRXN1-a* del DIFF cells. Further, we saw IP for neurons were equally distributed between individuals while IP for astroglia had more Ctrl-7 NES cells and immature cells had higher proportion originating from *NRXN1-a* del cells. Finally, we saw that Ctrl-7 DIFF contributed to neuronal cells and *NRXN1-a* del DIFF contributed to astroglia/non-neuronal cells (Fig. 3D).

Looking at individual genes differentially expressed over pseudotime and branches, we observed robust enrichment of neuronal genes (e.g *DCX, NCAM1, ROBO3, SYT4*) in the neuron branch and non-neuronal genes (e.g *APOE, COL6A3, MGP, PDGFRB*) in the astroglia branch (Fig. 3E and F). To validate our single cell observation we used Western blot and immunocytochemistry to probe for neuronal markers B3-tubulin and astroglial markers S100B, GFAP and FABP7 in our healthy control lines, and two additional *NRXN1-a* del NES clone cell lines and detected higher levels of astroglial related protein expression in differentiated *NRXN1-a* del cells at 28 days of differentiation (Fig. 3G and Fig. S3C).

Altogether our observations indicate that control NES cells at 28 days without growth factors predominantly differentiate towards neuronal cells (~90%) and lesser extent non-neuronal cells (~10%) while *NRXN1-a* del NES cells differentiate towards neuronal (~50%) and non-neuronal cells (~50%) adding up that *NRXN1-a* indeed plays a significant role in NES cell differentiation.

2.4. NRXN1-a deletion affects neuronal maturation and impairs emergence of excitatory neurons

We were further interested in studying the neuronal differentiation in Ctrl-7 and *NRXN1-a* del DIFF cells and looked into subset of immature neurons and neurons identified by BackSPIN (Fig. 4A). In the neuronal subtypes, we identified differentially expressed genes over three branches (Fig. S4A, Table S3) separating immature neurons and neuronal subtypes into inhibitory and excitatory neurons (Fig. 4B). We employed pseudotime ordering to estimate neuronal maturation and observed bifurcation point along the trajectory root branch coinciding with separation of neuronal subtypes (Fig. 4C and D). We selected genes for visualization of enrichment along the branches and displayed genes for immature (e.g. *FABP7, HES6, NEUROG1*), inhibitory (e.g. *CNTN2, GABRG1, GAD1*) and excitatory neurons (e.g. *CHRNA2, GRM5, RBFOX1*) (Fig. 4E). Separately plotting trajectories for Ctrl-7 and *NRXN1-a* del cells, we noted distribution differences in neuronal subtypes (Fig. 4F panel) and counting cells assigned to branches we observed Ctrl-7 cells consisting of 16% immature neurons, 35% inhibitory neurons and 49% excitatory neurons while *NRXN1-a* del cells consisted of 56% immature neurons, 33% inhibitory neurons and 11% excitatory neurons (Fig. 4G panel). These observed differences in neuronal subtype distribution suggested NRXN1-a del neurons being vastly different to the healthy control neurons at 28 days of differentiation.

Following up on observations in single cells, we validated immature neuronal identity in bulk differentiation samples with qPCR Taqman array against a panel of neurotransmitters. Here, we observed significant decrease in mRNA expression in *NRXN1-a* del DIFF cells when compared to healthy control DIFF cells (Fig. S4H).

These observations further led us to test functionality by calcium signaling and electrophysiological property. We considered *NRXN1* previously described as a presynaptic protein playing an essential role in synaptic transmission and voltage gated calcium channels play a major role in synaptic vesicle release [12]. We interrogated calcium signaling and recorded clear differences in calcium concentration $[Ca^{2+}]_i$ responses to depolarizing concentrations of KCl between Ctrl-7 and *NRXN1-a* del cells at both 28 days and 49 days of differentiation,

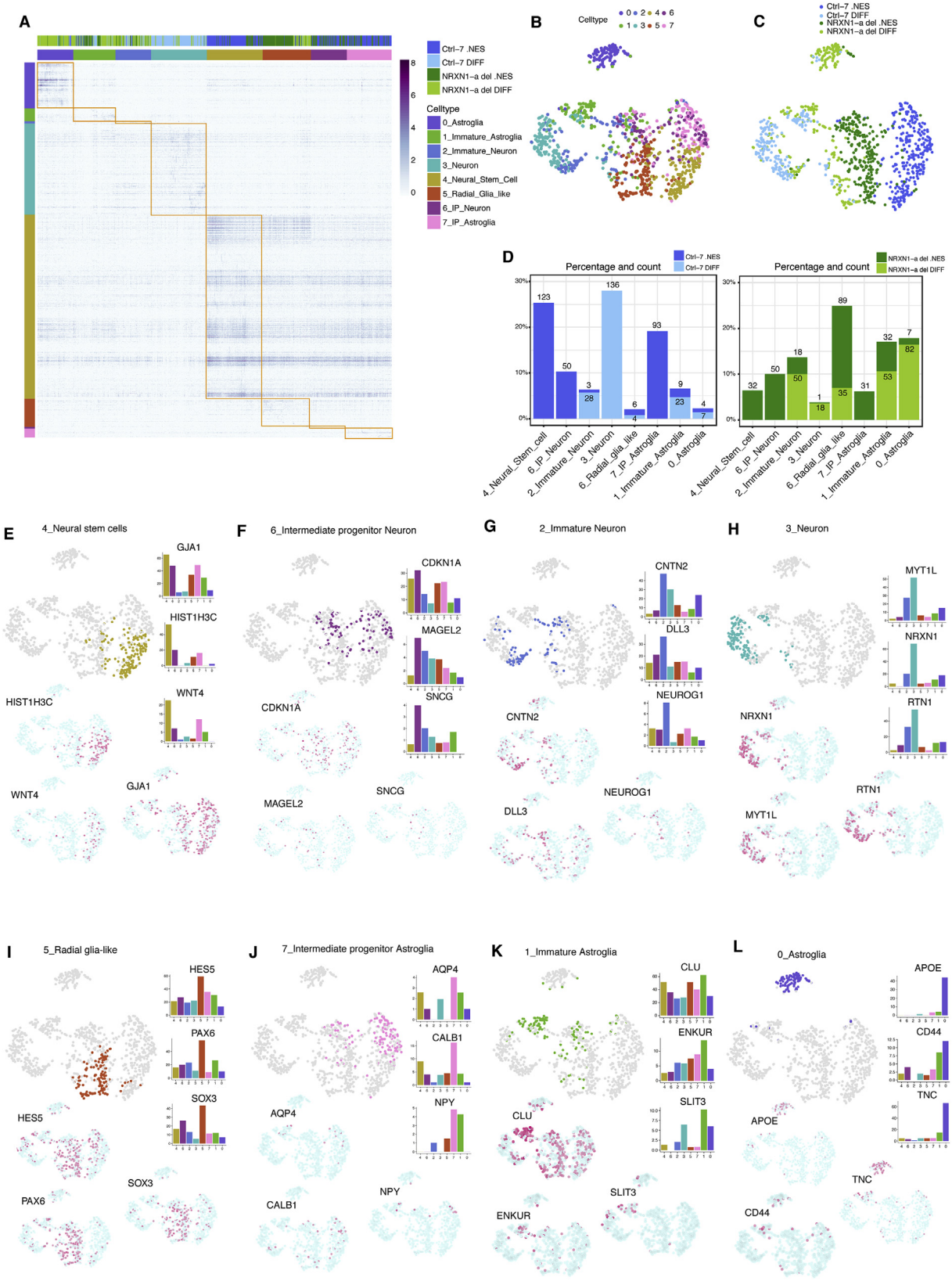

Fig. 2. BackSPIN clustering reveal cell types and cell type distribution differences between control cells and *NRXN1-a* del cells. A) Heatmap of 2000 most variable and enriched genes identified by BackSPIN resolving cell types, rows represent genes and columns represent cells, see Table 1 for genes corresponding to cell types (clusters). B) TSNE plot display clustering of cell types (8 clusters). C) TSNE plot display location of cell conditions. D) Barplots over cell count and percentage of cell types ordered to separate between sequential neuronal development and astroglia development. (Panels *E*–L: TSNE plots for cells expressing gene, barplots over percentage of cells expressing gene in cell types). E) Neural stem cell enriched genes: *GJA1, HIST1H3C, WNT4*. F) Intermediate progenitor for neurons enriched genes: CDKN1A, MAGEL2, SNCG. G) Immature neurons enriched genes: *CNTN2, DLL3, NEUROG1*. H) Neurons enriched genes: *MYT1L, NRXN1, RTN1*. I) Radial glia-like cells enriched genes: *HES5, PAX6, SOX3*. J) Intermediate progenitor for astroglia enriched genes: *AQP4, CALB1, NPY*. K) Immature astroglia enriched genes: *CLU, ENKUR, SLIT3*. L) Astroglia enriched genes: *APOE, CD44, TNC*.

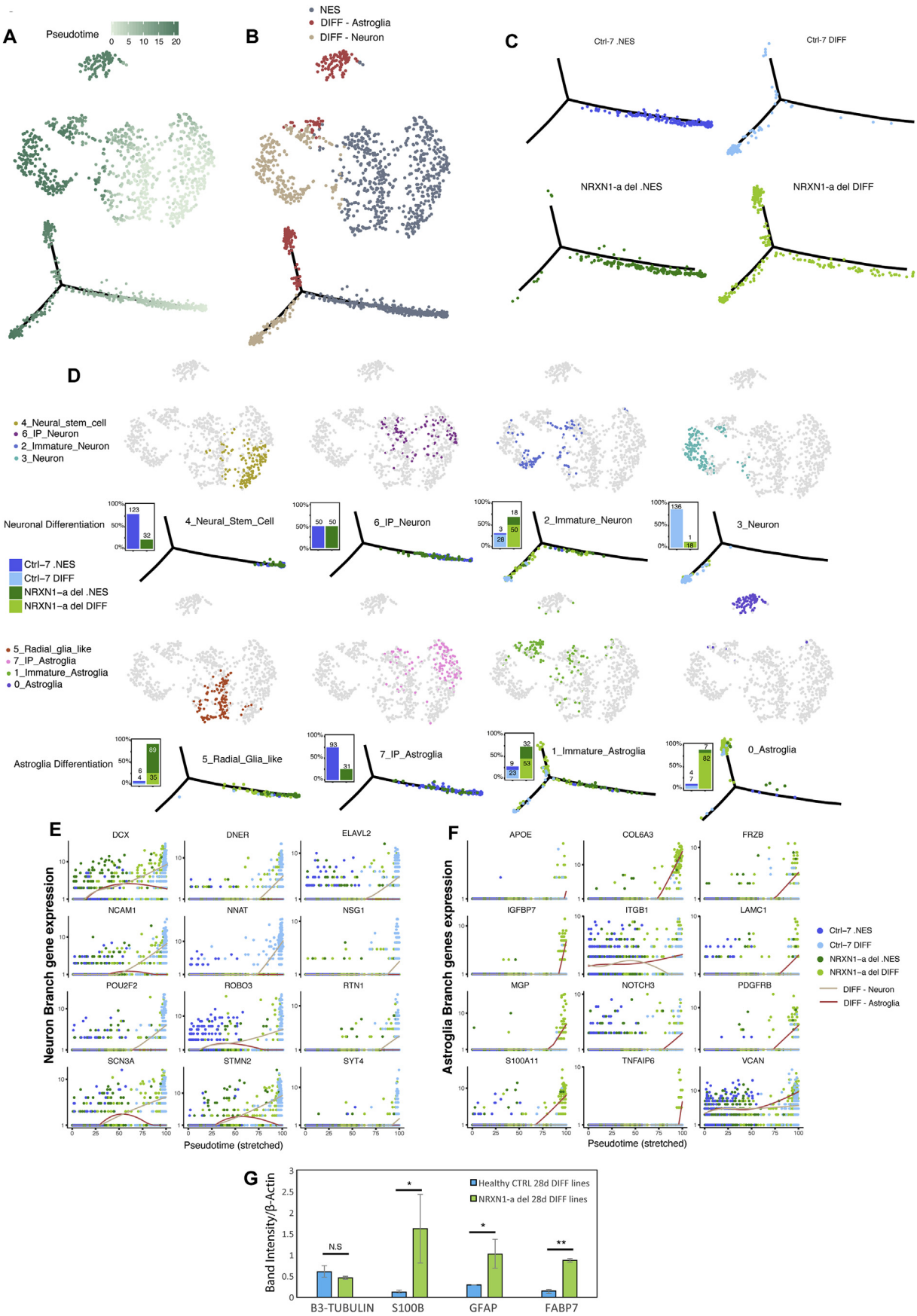

(caption on next page)

Fig. 3. Pseudotime and trajectory modeling reveal *NRXN1-a* deletion results in higher proportion astroglia in differentiated cells. A) TSNE and trajectory plot for pseudotime ordering of cells. B) TSNE and trajectory plot for branch identity, NES (grey), neurons (beige) and astroglia (red). C) Trajectory plots showing cell condition separated by individual and display cell condition aggregation along branches. D) Plots showing cell type aggregation in TSNE, aggregation along trajectory and percentage plus cell count in barplots. E) Neuronal gene expression over pseudotime showing branch dominant genes. F) Astroglia (non-neuronal) gene expression over pseudotime showing branch dominant genes. G) Densitometry summary for healthy control lines (Ctrl-7, Ctrl-3, Ctrl-9 and Ctrl-10) and *NRXN1-a* del clone cell lines (*NRXN1-a* del, *NRXN1-a* del SC, *NRXN1-a* del F) for S100B, GFAP and FABP7 protein show higher astroglia related protein presence in *NRXN1-a* del DIFF cells compared to control DIFF cells. . (For interpretation of the references to color in this figure legend, the reader is referred to the Web version of this article.)

here *NRXN1-a* del cells had significantly lower amplitude and slower rise time (Fig. 4H, I and 4J).

Next, we investigated electrophysiological properties and patched responsive neurons at 70–75 days of differentiation. Here, we disentangled neuron maturation stages by significant differences in action potential amplitude (APA) for both Ctrl-7 neurons and *NRXN1-a* del neurons. We classified maturation stages by immature (APA below 95 mV), intermediate mature (APA between 95 mV and 110 mV) and mature (APA above 110 mV) neurons and observed Ctrl-7 neurons separating into immature, intermediate and mature neurons. In contrast, *NRXN1-a* del neurons were observed only in immature neurons, intermediate mature neurons and no mature neurons (Fig. 4K, L and 4 M). Similarly, when we looked at timing of action potential profile across patched neurons, we observed a clear yet non-significant trend relation between maturation properties by amplitude height and speed of action potential peak time (Fig 4N).

Our observations of depressed calcium signaling capacity, lower levels of neurotransmitter detected and emergence of maturation impairment in *NRXN1-a* del neurons indicate proof of dysfunction present and detectable in our *NRXN1-a* deletion ASD disease model.

As we identified functional differences in the potential for calcium signaling in *NRXN1-a* del neurons, we thought of analyzing other candidate genes with known cell adhesive function (*CHL1, CNTN4, CNTN6, NLGN1*) and described as contributing to disease burden of ASD [35]. We used the STRING database [36] and looked for *NRXN1* interaction and found evidence for co-expression and interaction in other model organism, thus indicating evolutionary conserved function and mechanism between *NRXN1* and the other candidate genes (Fig. S4B). We probed single cell transcriptome and bulk samples and found no *CHL1* and *CNTN4* expression in *NRXN1-a* del NES or DIFF cells (Figs. S4C–S4D) and confirmed protein absence of CHL1 in *NRXN1-a* del cells during neuronal differentiation (Fig. S4E).

These observations suggest that *NRXN1-a* holds a key role for neuronal maturation and proposes deletion of *NRXN1-a* lead to skewed differentiation of NES cells into immature and inhibitory neurons as opposed to mature, functional inhibitory neurons and excitatory neurons during healthy neurogenesis.

3. Discussion

In the current study, we characterized the cellular properties of NES cells and neuronal cells from an individual with autism spectrum disorder carrying a bi-allelic *NRXN1*-alpha deletion. As a synaptic adhesion molecule, NRXN1 has been extensively investigated in interesting studies of synaptic transmission and neurotransmitter release in late stages of human neurogenesis [5,37]. Here, we propose a novel role for *NRXN1-a* during early neurogenesis that affects cell identity of NES cells and alters outcome in character and maturation of differentiated neuronal cells.

In our study, we observed two waves of *NRXN1* expression during neurogenesis, first during neural induction of iPS cells (Fig. 1B) and second during neuronal differentiation (Fig. 1E and F). In addition to differences in *NRXN1-a* expression between Ctrl-7 and *NRXN1-a* del cells, we observed, *NRXN1-a* del NES cells having a significantly lower proliferation capability, expressing radial glia-like genes and preferentially differentiating to astroglia (Figs. 1D, 2I and 2L and 3). These observations align with previous description of mammalian radial glia cells transforming into astrocytes [38]. Our results suggest *NRXN1-a* holds functional role during neural induction and during the establishment of neural stem cells.

When we looked at neuronal cell adhesion molecules implicated in ASD and interactors of *NRXN1* [35] (*CNTN4*, *CNTN6*, *NLGN1*, *CHL1*) (Fig. S4B) we observed comparable gene expression profiles in Cortecon [25] displaying peaks during neural induction (Fig. S4F). This suggests *NRXN1* form cell-to-cell adhesion complexes transiently during neural induction to achieve close proximity between cells, possibly for enhanced signaling and structural integrity for establishment of structures like the neural rosette during in vitro induction culture. The enhanced cell-cell adhesion in the neural rosette mimics tight junctions of the developing neural tube during embryogenesis and the stem cell niche of the ventricular zone in developing brain and likely plays an essential part in providing a structurally supportive environment for efficient establishment and maintenance of neural stem cells.

Additionally, when looking at *NRXN1* expression in human preimplantation embryonic cells [26] we found *NRXN1* co-expressed with known interactors during early embryonic development (Fig. S4G). These cumulative observations suggest *NRXN1* presence not only in the synapse but also play an important part for the proper formation of the embryo, during early embryogenesis. Similarly, when we looked for *NRXN1* expression in spatial transcriptomics data of early mouse 7.5 embryo (http://www.picb.ac.cn/hanlab/itranscriptome) [39] and during the early Xenopus developmental stages in single cell RNA-seq data (https://kleintools.hms.harvard.edu/tools/currentDatasetsList_xenopus_v2.html) [40] we observed *NRXN1* expressed during late gastrulation along the primitive streak in the mouse embryo and during early neurulation in early Xenopus developmental stages. These observations explain our result of finding *NRXN1-a* expression during neural induction and link *NRXN1* to acting as an evolutionary conserved molecule (Fig. 1B).

Focusing on neuronal differentiation of *NRXN1-a* del DIFF cells, we saw absence of *NRXN1-a* suspends neuronal maturation and appear to support generation of excitatory neurons (Fig. 4G). Neurexin and neuroligin adhesion in Xenopus, a well-known neuronal maturation process resulting in dendritogenesis and synaptic maturation [41] together with action of *Nrxn1* adding strength to synaptic glutamatergic transmission in mouse [42] suggests conserved functionality for *NRNX1-a* in supporting maturation of neuronal cells and in our study specifically suggests excitatory neuronal cells.

Our functional Ca^{2+} signaling assay demonstrated significantly smaller Ca^{2+} amplitudes and slower rise time kinetics in the *NRXN1-a* del DIFF cells (Fig. 4H–I and supporting movie 1) suggesting the depression (or absence) of expression of electrically excitable ion channels that are hallmarks of differentiated/mature neurons (i.e. voltage dependent Ca^{2+} channels, $Na+/K+$ voltage dependent channels, and transporters/exchangers). Despite higher abundance of non-neuronal *NRXN1-a* del DIFF cells (50% of the cells), the wide spread depression in the rise time kinetics of the calcium amplitude seen in all *NRXN1-a* del DIFF cells, suggests disruption in Ca^{2+} signaling being a direct result of *NRXN1-a* deficiency in both neuronal and non-neuronal cells. These observations link support to our observation of *NRXN1-a* del DIFF cells not maturing and remain immature, thus becoming predominantly immature neurons (Figs. 3D, 4I and 4K, 4L and 4 M).

Supplementary video related to this article can be found at https://doi.org/10.1016/j.yexcr.2019.06.014.

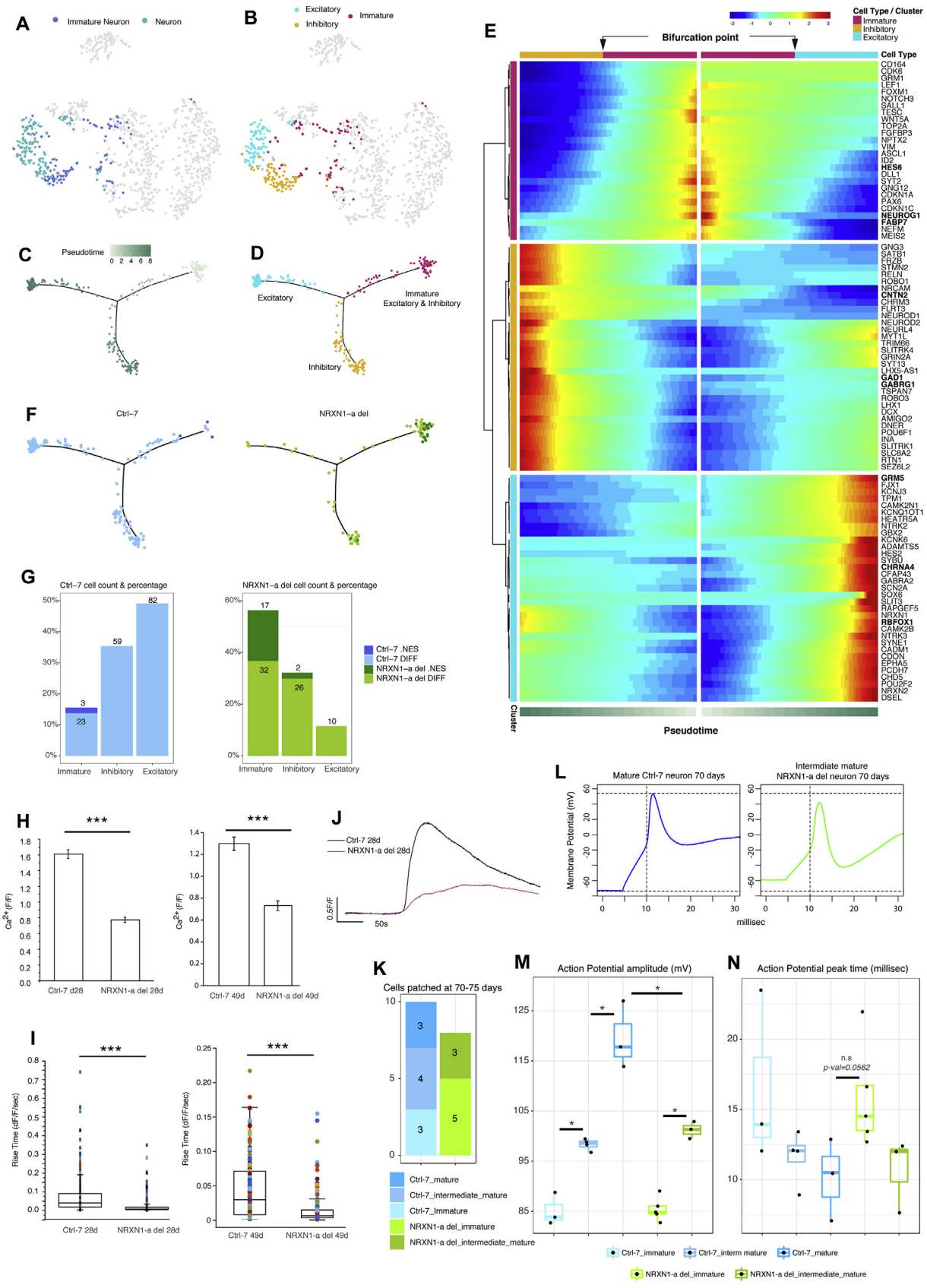

(caption on next page)

Fig. 4. *NRXN1-a* deletion affects neuronal maturation and impairs emergence of excitatory neurons. A) TSNE plot highlights immature neuron and neuron cell type. B) TSNE plot highlights three neuronal cell subtypes (immature, excitatory and inhibitory neurons). C) Pseudotime ordering trajectory of immature and neuronal cell subtype. D) Trajectory of neuronal cell subtype, immature neuron excitatory and inhibitory neuron. E) Heatmap of branched gene expression over pseudotime, showing selected branch enriched genes, identifying immature neuron, inhibitory neuron and excitatory neuron expression profiles. F) Trajectory plots separated by individual, showing neuronal cell subtype aggregation along branches. G) Bar plots showing cell count and percentage of cell condition per individual, Ctrl-7 cells are aggregated along inhibitory and excitatory neuron branches, *NRXN1-a* del cells are aggregated mostly to immature and inhibitory neuron branches. H) Comparison of the Ca^{2+} amplitudes to depolarizing concentrations of KCl (10 mM) between Ctrl-7 28d DIFF (n = 405, N = 3) and *NRXN1-a* 28d DIFF (n = 307, N = 3) cells and for Ctrl-7 49d DIFF (n = 180, N = 2) and *NRXN1-a* 49d DIFF (n = 202, N = 2). P-value < 0.001. I) Rise time kinetics of the Ca^{2+} signal (20–80%) for Ctrl-7 28d DIFF (n = 405, N = 3) and *NRXN1-a* 28d DIFF (n = 307, N = 3) and of the Ca^{2+} signal (0.05–100%) for Ctrl-7 49d DIFF (n = 180, N = 2) and *NRXN1-a* 49d DIFF (n = 202, N = 2). *** = P-value < 0.001. J) Representative Ca^{2+} traces to depolarizing concentrations of KCl (10 mM), showing significantly smaller amplitudes (H) and slower rise time (I) in *NRXN1-a* DIFF compared to Ctrl-7 DIFF. Traces represent the mean of Ctrl-7 DIFF (n = 118, N = 1) and *NRXN1-a* DIFF (n = 79, N = 1) cells. K) Responsive patched cells acquired at 70–75 days of differentiation, cells classified with threshold set for maturity at action potential amplitude, below 95 mV Ctrl-7 immature neurons and *NRXN1-a* del immature neurons, between 95mV and 110mV Ctrl-7 intermediate neurons and *NRXN1-a* del intermediate mature neurons and above 110 mV Ctrl-7 mature neurons, no *NRXN1-a* del neurons reached above 110 mV at sampled 70–75 day time point. L) Representative action potential traces neurons differentiated for 70–75 days. Current injection (95 pA) invoked action potential and peak time (~7–12msec) in both Ctrl-7 neurons and *NRXN1-a* del neurons. Amplitude in Ctrl-7 mature neuron was consistently higher when compared to amplitude in *NRXN1-a* del intermediate mature neuron. Horizontal grid lines show beginning and peak of action potential for Ctrl-7 neuron, vertical grid line shows action potential reaching threshold at −20mV. M) Action potential amplitude was used to classify maturity, paired and unpaired *t*-test showed significant differences between all maturation stages both internally between all stages of Ctrl-7 neurons and *NRXN1-a* del neurons and across mature Ctrl-7 neurons and intermediate mature *NRXN1-a* del neurons, * = P-Value < 0.05. N) Action potential peaking times across maturation stages show a clear trend in low action potential amplitude corresponding slow action potential peak time. Largest difference seen between mature Ctrl-7 neurons and immature *NRXN1-a* del neurons (non-significant P-Value = 0.0562).

Our observations are consistent with studies where pan-neurexin deletion in mouse displayed decreased Ca^{2+} -triggered neurotransmitter release and decreased action-potential evoked presynaptic Ca^{2+} transients [12,14], aiding explanation to our *NRXN1-a* deletion ASD disease model is indeed recapitulating neuronal dysfunction. Validation of our ASD disease model is supported by two recent high impact studies reporting synaptic gene dys-regulation and astroglial gene up-regulation in postmortem ASD cerebral cortex [43,44]. Others working with human iPS derived ASD neuronal cells have reported observations similar to ours with enrichment of astroglia, dysregulated calcium activity and hypoexcitability in neurons [45,46].

To address limitations, we make note that our observations come from disease modeling one very rare individual carrying a complete biallelic *NRXN-a* deletion of *NRXN1-a.* Herein also lay our strength in the ability of precisely study the effects of a complete deletion of *NRXN1-a.*

Taken together, our results suggest cell properties of healthy control neural stem cells and neurons stand in stark contrast to cell properties of neural stem cells and neurons with a complete deletion of *NRXN1-a*. In conclusion, we propose *NRXN1-a* plays a pivotal role in the establishment of functionally efficient neural stem cells and *NRXN1-a* contributes to functional property and maturation in neurons.

Acknowledgments

We are deeply grateful to the patient and her family for participating in this study. The study was supported by Stiftelsen för strategisk forskning, SSF (IB13-0074 (AF)), the Swedish Research Council, Vetenskapsrådet 2015–02424 (ND), D0886501 (PFS) and 2017–03407 (AF), Sävstaholm Society (ND) and Karolinska Institutet Doctoral funding (ML). The authors thank the iPS Core (ipscore.se), ESCG (escg.se) facilities at Karolinska Institutet. ML especially acknowledges Åsa Björklund at the National Bioinformatics Infrastructure Sweden at SciLifeLab for bioinformatics advice. Jahan Salma contributed with very limited technical assistance.

Appendix A. Supplementary data

Supplementary data to this article can be found online at https://doi.org/10.1016/j.yexcr.2019.06.014.

Author contributions

Conceptualization, A.F. and P.F.S.; Methodology, M.L, M.M., J.B., R.J.P., E.U., L.L., J.O., R.M., H.R., I.D.E, L.L., N.D., P.U., B-M.A, M.K, P.F.S. and A.F.; Formal Analysis, M.L M.M, J.B, E.U., L.L., J.O., R.M., I.D.E., L.L. and S.V.K.,; Investigation, M.L, M.M., J.B., L.L., J.O., I.D.E. and L.L.; Resources, N.D., P.U., B-M.A, M.K, P.F.S. and A.F.; Data Curation, M.L., M.M., J.B. L.L, and I.D.E.; Validation, M.L., M.M., J.B., E.U., L.L., R.M., I.D.E., and M.K.; Writing – Original Draft, M.L., M.M., J.B. and A.F.; Writing – Review & Editing, M.L., M.M., J.B., R.J.P., E.U., L.L., J.O., R.M., H.R., I.D.E., L.L., N.D., P.U., B-M.A., M.K., P.F.S. and A.F.; Visualization, M.L., M.M., J.B., J.O., R.M., I.D.E., L.L. and M.K.; Supervision, N.D., P.U., M.K., P.F.S. and A.F.; Project Administration, M.K., P.F.S. and A.F.; Funding Acquisition N.D., P.U., B-M.A., P.F.S. and A.F.

Declaration of interest

The authors declare no conflict of interest.

Data availability

Processed data sets are available at: ArrayExpress accession E-MTAB-7744.

”QC_meta_data_summary_984_cells_with_BackSPIN_cell_annotation.txt” meta data for all 984 high quality single cells included in study.

”Expression_data_984_cells_13918_genes.txt” contain 984 high quality single cells and 13918 genes filtered according to criteria in methods section.

”Expression_data_984_cells_BackSPIN_2000_genes.txt” contain 984 high quality cells and 2000 highly variable genes identified with BackSPIN algorithm.

”2000_BackSPIN_genes_cluster_annotation.txt” contain cell type/cluster annotation for highly variable genes identified with BackSPIN algorithm.

Due to General Data Protection Regulation (GDPR) access to human sequenced raw data is restricted and will be made available upon request through https://doi.org/10.17044/nbis/g000008.

References

[1] C. Richards, C. Jones, L. Groves, J. Moss, C. Oliver, Prevalence of autism spectrum disorder phenomenology in genetic disorders: a systematic review and meta-analysis, Lancet Psychiatry 2 (2015) 909–916.
[2] A.V. Buescher, Z. Cidav, M. Knapp, D.S. Mandell, Costs of autism spectrum disorders in the United Kingdom and the United States, JAMA Pediatr 168 (2014) 721–728.
[3] M.C. Lai, M.V. Lombardo, S. Baron-Cohen, Autism. Lancet vol. 383, (2014) 896–910.
[4] C.Y. RK, D. Merico, M. Bookman, L.H. J, B. Thiruvahindrapuram, R.V. Patel, J. Whitney, N. Deflaux, J. Bingham, Z. Wang, et al., Whole genome sequencing

resource identifies 18 new candidate genes for autism spectrum disorder, Nat. Neurosci. 20 (2017) 602–611.
[5] C. Pak, T. Danko, Y. Zhang, J. Aoto, G. Anderson, S. Maxeiner, F. Yi, M. Wernig, T.C. Sudhof, Human neuropsychiatric disease modeling using conditional deletion reveals synaptic transmission defects caused by heterozygous mutations in NRXN1, Cell Stem Cell 17 (2015) 316–328.
[6] C.R. Marshall, D.P. Howrigan, D. Merico, B. Thiruvahindrapuram, W. Wu, D.S. Greer, D. Antaki, A. Shetty, P.A. Holmans, D. Pinto, et al., Contribution of copy number variants to schizophrenia from a genome-wide study of 41,321 subjects, Nat. Genet. 49 (2017) 27–35.
[7] J. de Wit, A. Ghosh, Specification of synaptic connectivity by cell surface interactions, Nat. Rev. Neurosci. 17 (2016) 22–35.
[8] A.K. Jenkins, C. Paterson, Y. Wang, T.M. Hyde, J.E. Kleinman, A.J. Law, Neurexin 1 (NRXN1) splice isoform expression during human neocortical development and aging, Mol. Psychiatry 21 (2016) 701–706.
[9] B. Ullrich, Y.A. Ushkaryov, T.C. Sudhof, Cartography of neurexins: more than 1000 isoforms generated by alternative splicing and expressed in distinct subsets of neurons, Neuron 14 (1995) 497–507.
[10] A.Y. Huang, D. Yu, L.K. Davis, J.H. Sul, F. Tsetsos, V. Ramensky, I. Zelaya, E.M. Ramos, L. Osiecki, J.A. Chen, et al., Rare copy number variants in NRXN1 and CNTN6 increase risk for tourette syndrome, Neuron 94 (2017) 1101–1111 e1107.
[11] G. Kirov, CNVs in neuropsychiatric disorders, Hum. Mol. Genet. 24 (2015) R45–R49.
[12] M. Missler, W. Zhang, A. Rohlmann, G. Kattenstroth, R.E. Hammer, K. Gottmann, T.C. Sudhof, Alpha-neurexins couple Ca2+ channels to synaptic vesicle exocytosis, Nature 423 (2003) 939–948.
[13] M.R. Etherton, C.A. Blaiss, C.M. Powell, T.C. Sudhof, Mouse neurexin-1alpha deletion causes correlated electrophysiological and behavioral changes consistent with cognitive impairments, Proc. Natl. Acad. Sci. U. S. A. 106 (2009) 17998–18003.
[14] L.Y. Chen, M. Jiang, B. Zhang, O. Gokce, T.C. Sudhof, Conditional deletion of all neurexins defines diversity of essential synaptic organizer functions for neurexins, Neuron 94 (2017) 611–625 e614.
[15] N. Fusaki, H. Ban, A. Nishiyama, K. Saeki, M. Hasegawa, Efficient induction of transgene-free human pluripotent stem cells using a vector based on Sendai virus, an RNA virus that does not integrate into the host genome, Proc. Jpn. Acad. Ser. B Phys. Biol. Sci. 85 (2009) 348–362.
[16] K. Takahashi, K. Tanabe, M. Ohnuki, M. Narita, T. Ichisaka, K. Tomoda, S. Yamanaka, Induction of pluripotent stem cells from adult human fibroblasts by defined factors, Cell 131 (2007) 861–872.
[17] F. Bena, D.L. Bruno, M. Eriksson, C. van Ravenswaaij-Arts, Z. Stark, T. Dijkhuizen, E. Gerkes, S. Gimelli, D. Ganesamoorthy, A.C. Thuresson, et al., Molecular and clinical characterization of 25 individuals with exonic deletions of NRXN1 and comprehensive review of the literature, Am J Med Genet B Neuropsychiatr Genet 162B (2013) 388–403.
[18] S. Islam, A. Zeisel, S. Joost, G. La Manno, P. Zajac, M. Kasper, P. Lonnerberg, S. Linnarsson, Quantitative single-cell RNA-seq with unique molecular identifiers, Nat. Methods 11 (2014) 163–166.
[19] M. Kele, K. Day, H. Ronnholm, J. Schuster, N. Dahl, A. Falk, Generation of human iPS cell line CTL07-II from human fibroblasts, under defined and xeno-free conditions, Stem Cell Res. 17 (2016) 474–478.
[20] E. Uhlin, H. Ronnholm, K. Day, M. Kele, K. Tammimies, S. Bolte, A. Falk, Derivation of human iPS cell lines from monozygotic twins in defined and xeno free conditions, Stem Cell Res. 18 (2017) 22–25.
[21] S. Wu, J. Johansson, P. Damdimopoulou, M. Shahsavani, A. Falk, O. Hovatta, A. Rising, Spider silk for xeno-free long-term self-renewal and differentiation of human pluripotent stem cells, Biomaterials 35 (2014) 8496–8502.
[22] A. Falk, P. Koch, J. Kesavan, Y. Takashima, J. Ladewig, M. Alexander, O. Wiskow, J. Tailor, M. Trotter, S. Pollard, et al., Capture of neuroepithelial-like stem cells from pluripotent stem cells provides a versatile system for in vitro production of human neurons, PLoS One 7 (2012) e29597.
[23] F.J. Muller, B.M. Schuldt, R. Williams, D. Mason, G. Altun, E.P. Papapetrou, S. Danner, J.E. Goldmann, A. Herbst, N.O. Schmidt, et al., A bioinformatic assay for pluripotency in human cells, Nat. Methods 8 (2011) 315–317.
[24] S.M. Chambers, C.A. Fasano, E.P. Papapetrou, M. Tomishima, M. Sadelain, L. Studer, Highly efficient neural conversion of human ES and iPS cells by dual inhibition of SMAD signaling, Nat. Biotechnol. 27 (2009) 275–280.
[25] J. van de Leemput, N.C. Boles, T.R. Kiehl, B. Corneo, P. Lederman, V. Menon, C. Lee, R.A. Martinez, B.P. Levi, C.L. Thompson, et al., CORTECON: a temporal transcriptome analysis of in vitro human cerebral cortex development from human embryonic stem cells, Neuron 83 (2014) 51–68.
[26] S. Petropoulos, D. Edsgard, B. Reinius, Q. Deng, S.P. Panula, S. Codeluppi, A. Plaza Reyes, S. Linnarsson, R. Sandberg, F. Lanner, Single-cell RNA-seq reveals lineage and X chromosome dynamics in human preimplantation embryos, Cell 165 (2016) 1012–1026.
[27] G. La Manno, D. Gyllborg, S. Codeluppi, K. Nishimura, C. Salto, A. Zeisel, L.E. Borm, S.R.W. Stott, E.M. Toledo, J.C. Villaescusa, et al., Molecular diversity of midbrain development in mouse, human, and stem cells, Cell 167 (2016) 566–580 e519.
[28] T.J. Nowakowski, A. Bhaduri, A.A. Pollen, B. Alvarado, M.A. Mostajo-Radji, E. Di Lullo, M. Haeussler, C. Sandoval-Espinosa, S.J. Liu, D. Velmeshev, et al., Spatiotemporal gene expression trajectories reveal developmental hierarchies of the human cortex, Science 358 (2017) 1318–1323.
[29] Y. Sun, W. Kong, A. Falk, J. Hu, L. Zhou, S. Pollard, A. Smith, CD133 (Prominin) negative human neural stem cells are clonogenic and tripotent, PLoS One 4 (2009) e5498.
[30] J. Tailor, R. Kittappa, K. Leto, M. Gates, M. Borel, O. Paulsen, S. Spitzer, R.T. Karadottir, F. Rossi, A. Falk, et al., Stem cells expanded from the human embryonic hindbrain stably retain regional specification and high neurogenic potency, J. Neurosci. 33 (2013) 12407–12422.
[31] A. Zeisel, A.B. Munoz-Manchado, S. Codeluppi, P. Lonnerberg, G. La Manno, A. Jureus, S. Marques, H. Munguba, L. He, C. Betsholtz, et al., Brain structure. Cell types in the mouse cortex and hippocampus revealed by single-cell RNA-seq, Science 347 (2015) 1138–1142.
[32] S.M. Chambers, Highly efficient neural conversion of human ES and iPS cells by dual inhibition of SMAD signaling, Nat. Biotechnol. 27 (2009) 275–280.
[33] L.v.d. Maaten, G.E. Hinton, Y. Bengio, Visualizing Data using t-SNE, J. Mach. Learn. Res. 9 (2008) 2579–2605.
[34] X. Qiu, Q. Mao, Y. Tang, L. Wang, R. Chawla, H.A. Pliner, C. Trapnell, Reversed graph embedding resolves complex single-cell trajectories, Nat. Methods 14 (2017) 979–982.
[35] J.M. Berg, D.H. Geschwind, Autism genetics: searching for specificity and convergence, Genome Biol. 13 (2012) 247.
[36] D. Szklarczyk, A. Franceschini, S. Wyder, K. Forslund, D. Heller, J. Huerta-Cepas, M. Simonovic, A. Roth, A. Santos, K.P. Tsafou, et al., STRING v10: protein-protein interaction networks, integrated over the tree of life, Nucleic Acids Res. 43 (2015) D447–D452.
[37] L. Zeng, P. Zhang, L. Shi, V. Yamamoto, W. Lu, K. Wang, Functional impacts of NRXN1 knockdown on neurodevelopment in stem cell models, PLoS One 8 (2013) e59685.
[38] A. Kriegstein, A. Alvarez-Buylla, The glial nature of embryonic and adult neural stem cells, Annu. Rev. Neurosci. 32 (2009) 149–184.
[39] G. Peng, S. Suo, J. Chen, W. Chen, C. Liu, F. Yu, R. Wang, S. Chen, N. Sun, G. Cui, et al., Spatial transcriptome for the molecular annotation of lineage fates and cell identity in mid-gastrula mouse embryo, Dev. Cell 36 (2016) 681–697.
[40] C.W. James A Briggs, D.E. Wagner, S. Megason, L. Peshkin, M.W. Kirschner, A.M. Klein, The dynamics of gene expression in vertebrate embryogenesis at single-cell resolution, Science 360 (6392) (2018).
[41] S.X. Chen, P.K. Tari, K. She, K. Haas, Neurexin-neuroligin cell adhesion complexes contribute to synaptotropic dendritogenesis via growth stabilization mechanisms in vivo, Neuron 67 (2010) 967–983.
[42] L.G. Rabaneda, E. Robles-Lanuza, J.L. Nieto-Gonzalez, F.G. Scholl, Neurexin dysfunction in adult neurons results in autistic-like behavior in mice, Cell Rep. 8 (2014) 338–346.
[43] M.J. Gandal, J.R. Haney, N.N. Parikshak, V. Leppa, G. Ramaswami, C. Hartl, A.J. Schork, V. Appadurai, A. Buil, T.M. Werge, et al., Shared molecular neuropathology across major psychiatric disorders parallels polygenic overlap, Science 359 (2018) 693–697.
[44] D. Velmeshev, L. Schirmer, D. Jung, M. Haeussler, Y. Perez, S. Mayer, A. Bhaduri, N. Goyal, D.H. Rowitch, A.R. Kriegstein, Single-cell genomics identifies cell type-specific molecular changes in autism, Science 364 (2019) 685–689.
[45] B.A. DeRosa, J. El Hokayem, E. Artimovich, C. Garcia-Serje, A.W. Phillips, D. Van Booven, J.E. Nestor, L. Wang, M.L. Cuccaro, J.M. Vance, et al., Convergent pathways in idiopathic autism revealed by time course transcriptomic analysis of patient-derived neurons, Sci. Rep. 8 (2018) 8423.
[46] M. Sundberg, I. Tochitsky, D.E. Buchholz, K. Winden, V. Kujala, K. Kapur, D. Cataltepe, D. Turner, M.J. Han, C.J. Woolf, et al., Purkinje cells derived from TSC patients display hypoexcitability and synaptic deficits associated with reduced FMRP levels and reversed by rapamycin, Mol. Psychiatry 23 (2018) 2167–2183.